

Sidearm Effects. Synthesis, Structural Characterization, and Reactivity of Lanthanides Incorporating a Linked Carboranyl-Indenyl Ligand with a Tethered Amine Group

Shaowu Wang,^{†,‡} Hung-Wing Li,[†] and Zuowei Xie^{*,†}

Department of Chemistry, The Chinese University of Hong Kong, Shatin, New Territories, Hong Kong, China, and Institute of Organic Chemistry, School of Chemistry and Materials Science, Anhui Normal University, Wuhu, Anhui 241000, China

Received March 30, 2004

A new amine-functionalized carboranyl-indenyl hybrid ligand shows unique properties in stabilizing various kinds of lanthanocene chloride complexes via increasing steric effects imposed by the coordination of NMe₂ to the central metal ion, leading to the isolation of kinetic products and monomeric neutral species. Treatment of Me₂SiCl(C₉H₆CH₂CH₂NMe₂) with 1 equiv of Li₂C₂B₁₀H₁₀ afforded the monolithium salt [Me₂Si(C₉H₅CH₂CH₂NMe₂)(C₂B₁₀H₁₁)]Li(OEt₂) (**2**). Interaction of **2** with 1 equiv of *n*-BuLi produced the dilithium salt [Me₂Si(C₉H₅CH₂CH₂NMe₂)(C₂B₁₀H₁₀)]Li₂(OEt₂)₂ (**3**). Treatment of **3** with 1 equiv of YbCl₃ gave [{η⁵:η¹:σ-Me₂Si(C₉H₅CH₂CH₂NMe₂)(C₂B₁₀H₁₀)}YbCl₂][Li(THF)₄] (**4**). Upon heating, **4** was converted to [{η⁵:η¹:σ-Me₂Si(C₉H₅CH₂CH₂NMe₂)(C₂B₁₀H₁₀)}Yb(μ-Cl)_{1.5}]₂[Li(THF)₄] (**6**) and finally to [{η⁵:η¹:σ-Me₂Si(C₉H₅CH₂CH₂NMe₂)(C₂B₁₀H₁₀)}Yb(μ-Cl)]₂ (**7**) via the elimination of LiCl. Treatment of **6** or its Sm analogue **5** with 2 equiv of sodium amide gave [η⁵:η¹:σ-Me₂Si(C₉H₅CH₂CH₂NMe₂)(C₂B₁₀H₁₀)]Yb(NHC₆H₃-2,6-Pr'₂) (**9**) or [η⁵:η¹:σ-Me₂Si(C₉H₅CH₂CH₂NMe₂)(C₂B₁₀H₁₀)]Sm(μ-NHC₆H₃-2,6-Pr'₂)(μ-Cl)Li(THF) (**8**). An equimolar reaction of SmI₂ with **3** generated, after addition of LiCl, [{η⁵:η¹:η⁶-Me₂Si(C₉H₅CH₂CH₂NMe₂)(C₂B₁₀H₁₀)]Sm₂(μ-Cl)][Li(THF)₄] (**10**). In sharp contrast, a less reactive YbI₂ reacted with **3** in THF, producing only the salt metathesis product [η⁵:η¹:σ-Me₂Si(C₉H₅CH₂CH₂NMe₂)(C₂B₁₀H₁₀)]Yb(DME) (**11**). **11** reacted with 1 equiv of **3** to give the ionic complex [{(μ-η⁵:η²):η¹:σ-Me₂Si(C₉H₅CH₂CH₂NMe₂)(C₂B₁₀H₁₀)]₂Yb}{Li(THF)₂}₂ (**12**). All complexes were characterized by spectroscopic techniques and elemental analyses. Their structures were all further confirmed by single-crystal X-ray analyses.

Introduction

Cyclopentadienyl or indenyl ligands with Lewis base functionalities have found many applications in rare earth chemistry.^{1,2} Our very recent work shows that the ether substituent on the five-membered ring of the indenyl unit in linked carboranyl-indenyl hybrid ligands has significant effects on the stability and reactivity of the resulting organo-rare-earth complexes via temporarily and reversibly coordinating to the metal ion.³ Considering very high oxophilicity of lanthanides and the steric demands of OMe versus NMe₂, we have extended our research to amine-functionalized carboranyl-indenyl hybrid ligands. The results indicate that [Me₂Si(C₉H₅CH₂CH₂NMe₂)(C₂B₁₀H₁₀)]²⁻ exhibits some interesting features in coordination chemistry. In this

contribution, we report a full account on the synthesis, structural characterization, and reactivity of lanthanides derived from this new ligand.⁴ Similarities and differences between [Me₂Si(C₉H₅CH₂CH₂NMe₂)(C₂B₁₀H₁₀)]²⁻ and [Me₂Si(C₉H₅CH₂CH₂OMe)(C₂B₁₀H₁₀)]²⁻ in coordination chemistry are also discussed.

Experimental Section

General Procedures. All experiments were performed under an atmosphere of dry dinitrogen with the rigid exclusion of air and moisture using standard Schlenk or cannula techniques, or in a glovebox. All organic solvents were freshly distilled from sodium benzophenone ketyl immediately prior to use. LnI₂(THF)_x (Ln = Sm, Yb),⁵ C₉H₇CH₂CH₂NMe₂,⁶ 2,6-Pr'₂-C₆H₃NHNa,⁷ and Li₂C₂B₁₀H₁₀⁸ were prepared according to literature methods. All other chemicals were purchased from Aldrich Chemical Co. and used as received unless otherwise noted. Infrared spectra were obtained from KBr pellets prepared in the glovebox on a Perkin-Elmer 1600 Fourier

* Corresponding author. Fax: (852)26035057. Tel: (852)26096344. E-mail: zxie@cuhk.edu.hk.

[†] The Chinese University of Hong Kong.

[‡] Anhui Normal University.

(1) For recent reviews, see: (a) Arndt, S.; Okuda, J. *Chem. Rev.* **2002**, *102*, 1953. (b) Okuda, J. *J. Chem. Soc., Dalton Trans.* **2003**, 2367.

(2) For reviews, see: (a) Schumann, H.; Messe-Markscheffel, J. A.; Esser, L. *Chem. Rev.* **1995**, *95*, 865. (b) Edelman, F. T. In *Comprehensive Organometallic Chemistry II*; Abel, E. W., Stone, F. A. G., Wilkinson, G., Eds.; Pergamon: New York, 1995; Vol. 4, p 11.

(3) Wang, S.; Li, H.-W.; Xie, Z. *Organometallics* **2004**, *23*, 2469.

(4) For preliminary communication, see: Wang, S.; Li, H.-W.; Xie, Z. *Organometallics* **2001**, *20*, 3624.

(5) Girard, P.; Namy, J. L.; Kagan, H. B. *J. Am. Chem. Soc.* **1980**, *102*, 2693.

(6) Qian, C.; Li, H.; Sun, J.; Nie, W. *J. Organomet. Chem.* **1999**, *585*, 59.

(7) Chan, H.-S.; Li, H.-W.; Xie, Z. *Chem. Commun.* **2002**, 652.

transform spectrometer. ^1H and ^{13}C NMR spectra were recorded on a Bruker DPX 300 spectrometer at 300.13 and 75.47 MHz, respectively. ^{11}B NMR spectra were recorded on a Varian Inova 400 spectrometer at 128.32 MHz. All chemical shifts are reported in δ units with reference to the residual protons of the deuterated solvents for proton and carbon chemical shifts and to external $\text{BF}_3\cdot\text{OEt}_2$ (0.00 ppm) for boron chemical shifts. Elemental analyses were performed by MEDAC Ltd., U.K.

Preparation of $\text{Me}_2\text{Si}(\text{C}_9\text{H}_5\text{CH}_2\text{CH}_2\text{NMe}_2)\text{Cl}$ (1). To an Et_2O (200 mL) solution of $\text{Me}_2\text{NCH}_2\text{CH}_2\text{C}_9\text{H}_7$ (5.10 g, 0.027 mol) was slowly added a 1.60 M solution of *n*-BuLi in *n*-hexane (17.0 mL, 0.027 mol) at 0 °C, and the mixture was warmed to room temperature and stirred overnight. The resulting solution was then cooled to 0 °C, and Me_2SiCl_2 (14.0 mL, 0.108 mol) was quickly added in one portion. The mixture was stirred at room temperature overnight. The precipitate was filtered off. Removal of the solvent and excess Me_2SiCl_2 gave **1** as a pale yellow oil (6.60 g, 87%), which was pure enough for the next reaction step. ^1H NMR (CDCl_3): δ 7.55 (d, $J = 7.5$ Hz, 1H), 7.48 (d, $J = 7.5$ Hz, 1H), 7.32 (dd, $J = 7.5$ and 7.5 Hz, 1H), 7.23 (dd, $J = 7.5$ and 7.5 Hz, 1H), 6.36 (s, 1H), 3.64 (s, 1H) (C_9H_6), 2.92 (m, 2H), 2.78 (m, 2H), 2.49 (s, 6H) ($\text{CH}_2\text{CH}_2\text{N}(\text{CH}_3)_2$), 0.22 (s, 3H), 0.17 (s, 3H) ($\text{Si}(\text{CH}_3)_2$). ^{13}C NMR (CDCl_3): δ 144.80, 143.99, 141.52, 129.22, 126.29, 125.18, 124.06, 119.84, 45.48 (C_9H_6), 58.88, 46.40, 26.12 ($\text{CH}_2\text{CH}_2\text{N}(\text{CH}_3)_2$), 0.52, 0.43 ($\text{Si}(\text{CH}_3)_2$). MS (EI): 279 (M^+).

Preparation of $[\text{Me}_2\text{Si}(\text{C}_9\text{H}_5\text{CH}_2\text{CH}_2\text{NMe}_2)(\text{C}_2\text{B}_{10}\text{H}_{11})]\text{Li}(\text{OEt})_2$ (2). To a solution of *o*- $\text{C}_2\text{B}_{10}\text{H}_{12}$ (3.25 g, 22.6 mmol) in a dry toluene/diethyl ether (2:1, 20 mL) mixture was slowly added a 1.6 M solution of *n*-BuLi in hexane (28.5 mL, 45.6 mmol) at 0 °C, and the mixture was warmed to room temperature and stirred for 1 h. The resulting solution was then cooled to 0 °C, and a solution of **1** (6.33 g, 22.6 mmol) in a toluene/diethyl ether (2:1, 20 mL) mixture was slowly added. The mixture was stirred at room temperature for 25 h. After removal of the solvents, the resulting sticky solid was extracted with diethyl ether (20 mL \times 2). The ether solutions were combined and concentrated to give a pale yellow solid. This solid was washed with *n*-hexane (10 mL \times 2) and dried in a vacuum, affording **2** as a pale yellow solid (8.40 g, 79%). ^1H NMR (pyridine- d_5): δ 8.07 (d, $J = 7.8$ Hz, 1H), 7.92 (d, $J = 7.2$ Hz, 1H), 7.26 (s, 1H), 7.11 (m, 2H) (C_9H_5), 3.74 (br s, 1H) (cage CH), 3.48 (m, 2H), 2.93 (m, 2H), 3.28 (s, 6H) ($\text{CH}_2\text{CH}_2\text{N}(\text{CH}_3)_2$), 3.36 (q, $J = 7.2$ Hz, 4H), 1.12 (t, $J = 7.2$ Hz, 6H) ($\text{O}(\text{CH}_2\text{CH}_3)_2$), 0.81 (s, 6H) ($\text{Si}(\text{CH}_3)_2$). ^{13}C NMR (pyridine- d_5): δ 139.00, 133.23, 123.92, 121.10, 119.05, 116.23, 115.18, 110.82, 88.16 (C_9H_5), 63.22, 45.22, 26.33 ($\text{CH}_2\text{CH}_2\text{N}(\text{CH}_3)_2$), 79.11, 66.35 ($\text{C}_2\text{B}_{10}\text{H}_{11}$), 66.16, 15.61 ($\text{O}(\text{CH}_2\text{CH}_3)_2$), 1.55 ($\text{Si}(\text{CH}_3)_2$). ^{11}B NMR (pyridine- d_5): δ -5.05 (2), -10.45 (3), -14.49 (5). IR (KBr, cm^{-1}): ν_{BH} 2565 (vs). Anal. Calcd for $\text{C}_{17}\text{H}_{32}\text{B}_{10}\text{LiN}_2\text{O}_2$ (**2** - Et_2O): C, 51.88; H, 8.20; N, 3.56. Found: C, 52.05; H, 8.39; N, 3.38.

Preparation of $[\text{Me}_2\text{Si}(\text{C}_9\text{H}_5\text{CH}_2\text{CH}_2\text{NMe}_2)(\text{C}_2\text{B}_{10}\text{H}_{10})]\text{Li}_2(\text{OEt})_2$ (3). To a suspension of **2** (7.50 g, 16.0 mmol) in a mixed solvent of *n*-hexane and diethyl ether (2:1, 65 mL) was slowly added a 1.60 M solution of *n*-BuLi in hexane (10.5 mL, 16.8 mmol) at 0 °C, and the mixture was stirred at room temperature overnight. Removal of the solvent gave a yellow solid, which was washed with *n*-hexane (3 \times 15 mL), affording **3** as a pale yellow powder (7.90 g, 90%). ^1H NMR (pyridine- d_5): δ 8.16 (d, $J = 8.7$ Hz, 1H), 7.83 (d, $J = 8.7$ Hz, 1H), 7.34 (s, 1H), 7.06 (m, 2H) (C_9H_5), 3.18 (m, 2H), 2.54 (m, 2H), 2.16 (s, 6H) ($\text{CH}_2\text{CH}_2\text{N}(\text{CH}_3)_2$), 3.39 (m, 8H), 1.13 (m, 12H) ($\text{O}(\text{CH}_2\text{CH}_3)_2$), 0.83 (s, 6H) ($\text{Si}(\text{CH}_3)_2$). ^{13}C NMR (pyridine- d_5): δ 138.09, 132.79, 125.72, 122.20, 118.14, 115.43, 114.21, 110.89, 89.18 (C_9H_5), 62.62, 46.05, 27.25 ($\text{CH}_2\text{CH}_2\text{N}(\text{CH}_3)_2$), 78.18 ($\text{C}_2\text{B}_{10}\text{H}_{11}$), 66.17, 15.90 ($\text{O}(\text{CH}_2\text{CH}_3)_2$), 2.21 ($\text{Si}(\text{CH}_3)_2$). ^{11}B NMR (pyridine- d_5): δ 6.97 (1), 6.52 (1), 6.01 (1), 2.38 (2), -0.14 (4), -1.96 (1). IR (KBr, cm^{-1}): ν_{BH} 2556 (vs). Anal. Calcd for $\text{C}_{21}\text{H}_{41}\text{B}_{10}\text{Li}_2\text{NOSi}$ (**3** - Et_2O): C, 53.25; H, 8.73; N, 2.96. Found: C, 53.09; H, 8.69; N, 2.89.

Preparation of $[\{\eta^5\text{-}\eta^1\text{-}\sigma\text{-Me}_2\text{Si}(\text{C}_9\text{H}_5\text{CH}_2\text{CH}_2\text{NMe}_2)(\text{C}_2\text{B}_{10}\text{H}_{10})\}\text{YbCl}_2][\text{Li}(\text{THF})_4]$ (4). To a suspension of YbCl_3 (0.28 g, 1.0 mmol) in THF (20 mL) was slowly added a THF (10 mL) solution of **3** (0.55 g, 1.0 mmol) at room temperature. The reaction mixture was stirred at room temperature for 10 h. The color of the solution gradually changed from colorless to purple with disappearance of YbCl_3 . The solvent was removed under vacuum, affording a sticky purple solid, to which was added 15 mL of toluene. After removal of the precipitate, the clear solution was concentrated to about 10 mL. **4** was isolated as purple crystals after this solution stood at room temperature for 4 days (0.72 g, 78%). ^1H NMR (pyridine- d_5): δ 3.52 (s), 1.43 (s) (THF), plus 22.9 (br s), 13.6 (br s), 7.91 (s), 7.78 (s), 3.42 (s), 2.80 (s), 2.14 (s), 0.65 (s), -6.8 (br s), -13.6 (br s). ^{11}B NMR (pyridine- d_5): δ -2.98 (1), -7.51 (1), -10.76 (3), -20.19 (2), -29.06 (2), -61.32 (1). IR (KBr, cm^{-1}): ν_{BH} 2563 (vs). Anal. Calcd for $\text{C}_{29}\text{H}_{55}\text{B}_{10}\text{Cl}_2\text{LiNO}_3\text{SiYb}$ (**4** - THF): C, 40.84; H, 6.50; N, 1.64. Found: C, 41.11; H, 6.58; N, 1.51.

Preparation of $[\{\eta^5\text{-}\eta^1\text{-}\sigma\text{-Me}_2\text{Si}(\text{C}_9\text{H}_5\text{CH}_2\text{CH}_2\text{NMe}_2)(\text{C}_2\text{B}_{10}\text{H}_{10})\}\text{Sm}(\mu\text{-Cl})_{1.5}]_2[\text{Li}(\text{THF})_4]\cdot\text{THF}$ (5·THF). To a suspension of SmCl_3 (0.26 g, 1.0 mmol) in THF (15 mL) was slowly added a THF solution of **3** (0.55 g, 1.0 mmol) at room temperature, and the mixture was stirred overnight. The color of the solution changed gradually from colorless to orange with disappearance of SmCl_3 . After removal of the solvent, toluene (15 mL) was added to the sticky solid. The mixture was then stirred for 1 h, and the precipitate was filtered off. The clear solution was concentrated to about 10 mL. **5·THF** was isolated as orange-red crystals after this solution stood at room temperature for 4 days (0.49 g, 63%). ^1H NMR (pyridine- d_5): δ 3.66 (s), 1.64 (s) (THF), plus many broad, unresolved resonances. ^{11}B NMR (pyridine- d_5): δ -0.66 (2), -4.29 (4), -7.43 (4). IR (KBr, cm^{-1}): ν_{BH} 2554 (vs). Anal. Calcd for $\text{C}_{50}\text{H}_{94}\text{B}_{20}\text{Cl}_3\text{LiN}_2\text{O}_4\text{Si}_2\text{Sm}_2$ (**5**): C, 40.75; H, 6.43; N, 1.90. Found: C, 40.59; H, 6.31; N, 1.79.

Preparation of $[\{\eta^5\text{-}\eta^1\text{-}\sigma\text{-Me}_2\text{Si}(\text{C}_9\text{H}_5\text{CH}_2\text{CH}_2\text{NMe}_2)(\text{C}_2\text{B}_{10}\text{H}_{10})\}\text{Yb}(\mu\text{-Cl})_{1.5}]_2[\text{Li}(\text{THF})_4]\cdot\text{C}_7\text{H}_8$ (6·C₇H₈). A suspension of **4** (0.30 g, 0.32 mmol) in a mixed solvent of toluene/THF (7:1, 15 mL) was refluxed for 2 h. The white precipitate was filtered off. The clear solution was then concentrated to about 8 mL. **6·C₇H₈** was isolated as blue crystals after this solution stood at room temperature for 2 days (0.16 g, 62%). ^1H NMR (pyridine- d_5): δ 3.55 (s), 1.52 (s) (THF), plus many broad, unresolved resonances. ^{11}B NMR (pyridine- d_5): δ -1.39 (2), -6.43 (2), -12.82 (6). IR (KBr, cm^{-1}): ν_{BH} 2570 (vs). Anal. Calcd for $\text{C}_{46}\text{H}_{86}\text{B}_{20}\text{Cl}_3\text{LiN}_2\text{O}_3\text{Si}_2\text{Yb}_2$ (**6** - THF): C, 38.18; H, 5.99; N, 1.94. Found: C, 38.27; H, 6.10; N, 1.80.

Preparation of $[\{\eta^5\text{-}\eta^1\text{-}\sigma\text{-Me}_2\text{Si}(\text{C}_9\text{H}_5\text{CH}_2\text{CH}_2\text{NMe}_2)(\text{C}_2\text{B}_{10}\text{H}_{10})\}\text{Yb}(\mu\text{-Cl})_2]$ (7). A suspension of **6·C₇H₈** (0.26 g, 0.16 mmol) in a mixed solvent of toluene/THF (10:1, 15 mL) was refluxed for 6 h until all LiCl precipitated out. After removal of the white precipitate, the clear solution was then concentrated to about 10 mL. **7** was isolated as blue crystals after this solution stood at room temperature for 3 days (0.11 g, 58%). ^1H NMR (pyridine- d_5): δ 23.0 (s), 7.96 (d, $J = 7.2$ Hz), 7.83 (d, $J = 7.2$ Hz), 3.37 (br s), 2.82 (br s), 2.20 (s), 0.70 (s), -6.7 (br s), -13.6 (br s). ^{11}B NMR (pyridine- d_5): δ -3.51 (3), -8.72 (2), -14.44 (5). IR (KBr, cm^{-1}): ν_{BH} 2553 (vs). Anal. Calcd for $\text{C}_{34}\text{H}_{62}\text{B}_{20}\text{Cl}_2\text{N}_2\text{Si}_2\text{Yb}_2$: C, 34.37; H, 5.26; N, 2.36. Found: C, 34.18; H, 5.19; N, 2.18.

Preparation of $[\eta^5\text{-}\eta^1\text{-}\sigma\text{-Me}_2\text{Si}(\text{C}_9\text{H}_5\text{CH}_2\text{CH}_2\text{NMe}_2)(\text{C}_2\text{B}_{10}\text{H}_{10})]\text{Sm}(\mu\text{-NHC}_6\text{H}_3\text{-2,6-Pr}'_2)(\mu\text{-Cl})\text{Li}(\text{THF})$ (8). To a THF (15 mL) solution of **5·THF** (0.26 g, 0.17 mmol) was slowly added a THF (10 mL) solution of $\text{NaNHC}_6\text{H}_3\text{-2,6-Pr}'_2$ (0.067 g, 0.34 mmol) at room temperature, and the mixture was stirred overnight. After removal of the solvent, toluene (15 mL) was added to the resulting orange solid. The mixture was then refluxed for 1 h. The white precipitate was filtered off, and the clear orange solution was concentrated to about 8 mL. **8** was isolated as orange crystals after this solution stood at room temperature for 4 days (0.19 g, 68%). ^1H NMR (pyridine- d_5):

many broad, unresolved resonances. ^{11}B NMR (pyridine- d_5): δ -4.12 (1), -12.99 (9). IR (KBr, cm^{-1}): ν_{BH} 2546 (vs). Anal. Calcd for $\text{C}_{29}\text{H}_{49}\text{B}_{10}\text{ClLiN}_2\text{SiSm}$ (**8** - THF): C, 46.15; H, 6.54; N, 3.71. Found: C, 46.06; H, 6.61; N, 3.82.

Preparation of $[\eta^5\text{-}\eta^1\text{-}\sigma\text{-Me}_2\text{Si}(\text{C}_9\text{H}_5\text{CH}_2\text{CH}_2\text{NMe}_2)(\text{C}_2\text{B}_{10}\text{H}_{10})]\text{Yb}(\text{NHC}_6\text{H}_3\text{-2,6-Pr}'_2)\cdot 0.5\text{C}_6\text{H}_6$ (9**·0.5 C_6H_6).** This complex was prepared as purple crystals from **4** (0.30 g, 0.32 mmol) and $\text{NaNHC}_6\text{H}_3\text{-2,6-Pr}'_2$ (0.067 g, 0.34 mmol) in THF (25 mL) at room temperature using the procedure identical to that reported for **8** except for using benzene instead of toluene: yield 0.19 g (77%). ^1H NMR (pyridine- d_5): many broad, unresolved resonances. ^{11}B NMR (pyridine- d_5): δ 0.03 (1), -6.43 (1), -10.57 (2), -31.90 (6). IR (KBr, cm^{-1}): ν_{BH} 2562 (vs). Anal. Calcd for $\text{C}_{29}\text{H}_{49}\text{B}_{10}\text{N}_2\text{SiYb}$ (**9**): C, 47.39; H, 6.72; N, 3.81. Found: C, 47.15; H, 6.91; N, 3.66.

This complex was also prepared from the reaction of **6** or **7** with $\text{NaNHC}_6\text{H}_3\text{-2,6-Pr}'_2$ in 65% or 70% yield, respectively.

Preparation of $[(\eta^5\text{-}\eta^1\text{-}\eta^6\text{-Me}_2\text{Si}(\text{C}_9\text{H}_5\text{CH}_2\text{CH}_2\text{NMe}_2)(\text{C}_2\text{B}_{10}\text{H}_{10}))\text{Sm}_2(\mu\text{-Cl})][\text{Li}(\text{THF})_4]\cdot\text{C}_7\text{H}_8$ (10**· C_7H_8).** To a THF solution of $\text{SmI}_2(\text{THF})_x$ (9.5 mL, 1.0 mmol) was slowly added a THF solution of **3** (0.55 g, 1.0 mmol) at room temperature, to which was added LiCl (0.19 g, 4.5 mmol). The reaction mixture was then stirred at room temperature overnight. The color of the solution changed slowly from dark blue to purple. After removal of the solvent, the resulting sticky purple solid was washed with hot toluene (3×5 mL). The solid was then extracted with a mixed solvent of toluene and THF (10:1, 3×10 mL). The solutions were combined and concentrated to about 15 mL. **10**· C_7H_8 was isolated as dark red crystals after this solution stood at room temperature for a week (0.32 g, 43%). ^1H NMR (pyridine- d_5): δ 12.27 (br s), 11.72 (br s), 10.38 (d, $J = 6.0$ Hz), 10.17 (d, $J = 9.0$ Hz), 9.96 (br s), 7.83 (br s), 7.29 (m), 6.92 (br s), 6.01 (m), 5.73 (m), 5.63 (m), 3.66 (s), 2.87 (m), 2.68 (m), 2.18 (br s), 1.59 (s), 0.68 (br s), -0.01 (br s). ^{13}C NMR (pyridine- d_5): δ 147.77, 146.11, 142.24, 138.52, 134.74, 129.75, 128.99, 126.10, 124.81, 123.13, 120.45, 120.09, 119.26, 114.05, 90.16, 68.18, 59.83, 58.45, 45.87, 27.01, 26.15, 23.19, -0.37, -4.45. ^{11}B NMR (pyridine- d_5): δ -4.54 (4), -11.00 (4), -15.04 (8), -15.92 (4). IR (KBr, cm^{-1}): ν_{BH} 2527 (vs), 2444 (s). Anal. Calcd for $\text{C}_{42}\text{H}_{78}\text{B}_{20}\text{ClLi}_2\text{N}_2\text{O}_2\text{Si}_2\text{Sm}_2$ (**10** - 2THF): C, 40.08; H, 6.25; N, 2.23. Found: C, 39.75; H, 6.47; N, 2.50.

Preparation of $[\eta^5\text{-}\eta^1\text{-}\sigma\text{-Me}_2\text{Si}(\text{C}_9\text{H}_5\text{CH}_2\text{CH}_2\text{NMe}_2)(\text{C}_2\text{B}_{10}\text{H}_{10})]\text{Yb}(\text{DME})$ (11**).** To a THF solution of $\text{YbI}_2(\text{THF})_x$ (19.0 mL, 1.0 mmol) was slowly added a THF solution of **3** (0.55 g, 1.0 mmol) at room temperature, and the reaction mixture was then stirred overnight. The color of the solution changed from yellow to orange-red. After removal of the solvent, the oily residue was washed with hot toluene (3×5 mL). The resulting orange solid was then extracted with a mixed solvent of toluene and DME (10:1, 3×7 mL). The solutions were combined and concentrated to about 15 mL. **11** was isolated as orange crystals after this solution stood at room temperature for 3 days (0.43 g, 66%). ^1H NMR (pyridine- d_5): δ 8.23 (d, $J = 8.1$ Hz, 1H), 7.27 (d, $J = 7.2$ Hz, 1H), 7.19 (m, 2H), 7.02 (dd, $J = 7.2$ and 7.2 Hz, 1H) (C_9H_5), 2.84 (m, 2H), 2.52 (m, 2H), 2.07 (s, 6H) ($\text{CH}_2\text{CH}_2\text{N}(\text{CH}_3)_2$), 3.49 (m, 4H), 3.27 (s, 6H) (DME), 0.88 (s, 3H), 0.79 (s, 3H) ($\text{Si}(\text{CH}_3)_2$). ^{13}C NMR (pyridine- d_5): δ 134.78, 130.16, 126.35, 122.085, 120.79, 119.20, 118.68, 113.26, 98.24 (C_9H_5), 62.61, 45.93, 26.61 ($\text{CH}_2\text{CH}_2\text{N}(\text{CH}_3)_2$), 80.91, 68.21 ($\text{C}_2\text{B}_{10}\text{H}_{11}$), 72.41, 58.98 (DME), 0.92, 0.65 ($\text{Si}(\text{CH}_3)_2$). ^{11}B NMR (pyridine- d_5): δ -0.51 (1), -3.05 (3), -7.99 (6). IR (KBr, cm^{-1}): ν_{BH} 2547 (vs). Anal. Calcd for $\text{C}_{21}\text{H}_{41}\text{B}_{10}\text{NO}_2\text{SiYb}$: C, 38.88; H, 6.37; N, 2.16. Found: C, 38.69; H, 6.48; N, 2.14.

Preparation of $\{[(\mu\text{-}\eta^5\text{-}\eta^2\text{-}\eta^1\text{-}\sigma\text{-Me}_2\text{Si}(\text{C}_9\text{H}_5\text{CH}_2\text{CH}_2\text{NMe}_2)(\text{C}_2\text{B}_{10}\text{H}_{10}))_2\text{Yb}]\text{Li}(\text{THF})_2\}_2$ (12**).** To a THF (10 mL) solution of **11** (0.27 g, 0.42 mmol) was slowly added a THF (15 mL) solution of **3** (0.23 g, 0.42 mmol) at room temperature, and the mixture was stirred overnight. The color of the solution changed from orange to red. After removal of the solvent, the

oily residue was washed with hot toluene (2×10 mL). The resulting solid was then extracted with a mixed solvent of toluene and THF (10:1, 3×7 mL). The solutions were combined and concentrated to about 15 mL. **12** was obtained as red crystals after this solution stood at room temperature for 5 days (0.37 g, 71%). ^1H NMR (pyridine- d_5): δ 8.24 (m, 2H), 8.14 (m, 1H), 7.82 (m, 1H), 7.34 (s, 1H), 7.05 (m, 4H), 6.93 (s, 1H) (C_9H_5), 3.18 (m, 4H), 2.54 (m, 4H), 2.37 (s, 12H) ($\text{CH}_2\text{CH}_2\text{N}(\text{CH}_3)_2$), 3.65 (m, 16H), 1.62 (m, 16H) ($\text{C}_4\text{H}_8\text{O}$), 0.92 (s, 6H), 0.79 (s, 6H) ($\text{Si}(\text{CH}_3)_2$). ^{13}C NMR (pyridine- d_5): δ 139.21, 137.83, 135.73, 130.13, 127.14, 123.29, 120.25, 116.52, 112.48 (C_9H_5), 63.72, 47.32, 28.35 ($\text{CH}_2\text{CH}_2\text{N}(\text{CH}_3)_2$), 81.99, 64.32 ($\text{C}_2\text{B}_{10}\text{H}_{11}$), 69.31, 27.28 (THF), 2.02, 1.39 ($\text{Si}(\text{CH}_3)_2$). ^{11}B NMR (pyridine- d_5): δ -0.30 (2), -3.49 (6), -7.98 (12). IR (KBr, cm^{-1}): ν_{BH} 2564 (vs). Anal. Calcd for $\text{C}_{42}\text{H}_{78}\text{B}_{20}\text{Li}_2\text{N}_2\text{O}_2\text{Si}_2\text{Yb}$ (**12** - 2THF): C, 45.76; H, 7.13; N, 2.54. Found: C, 45.35; H, 7.37; N, 2.25.

This complex was directly prepared in 67% yield from the reaction of $\text{YbI}_2(\text{THF})_x$ with 2 equiv of **3**.

X-ray Structure Determination. All single crystals were immersed in Paratone-N oil and sealed under N_2 in thin-walled glass capillaries. Data were collected at 293 K on a Bruker SMART 1000 CCD diffractometer using Mo $\text{K}\alpha$ radiation. An empirical absorption correction was applied using the SADABS program.⁹ All structures were solved by direct methods and subsequent Fourier difference techniques and refined anisotropically for all non-hydrogen atoms by full-matrix least-squares calculations on F^2 using the SHELXTL program package.¹⁰ Most of the carborane hydrogen atoms were located from difference Fourier syntheses. All other hydrogen atoms were geometrically fixed using the riding model. Crystal data and details of data collection and structure refinements are given in Tables 1 and 2, respectively. Selected bond lengths and angles are compiled in Table 3. Further details are included in the Supporting Information.

Results and Discussion

Ligand. Reaction of $\text{Li}[\text{C}_9\text{H}_6\text{CH}_2\text{CH}_2\text{NMe}_2]$ with excess Me_2SiCl_2 in Et_2O gave $\text{Me}_2\text{SiCl}(\text{C}_9\text{H}_6\text{CH}_2\text{CH}_2\text{NMe}_2)$ (**1**) in 87% yield. Treatment of **1** with 1 equiv of $\text{Li}_2\text{C}_2\text{B}_{10}\text{H}_{10}$ in toluene/ Et_2O afforded the monolithium salt $[\text{Me}_2\text{Si}(\text{C}_9\text{H}_5\text{CH}_2\text{CH}_2\text{NMe}_2)(\text{C}_2\text{B}_{10}\text{H}_{11})]\text{Li}(\text{OEt}_2)$ (**2**) in 79% yield. Interaction of **2** with 1 equiv of $n\text{-BuLi}$ in Et_2O /hexane produced the dilithium salt $[\text{Me}_2\text{Si}(\text{C}_9\text{H}_5\text{CH}_2\text{CH}_2\text{NMe}_2)(\text{C}_2\text{B}_{10}\text{H}_{10})]\text{Li}_2(\text{OEt}_2)_2$ (**3**) in 90% yield. **3** is slightly soluble in ether, whereas **2** is highly soluble. Therefore, they were easily separated. These transformations are outlined in Scheme 1.

The ^1H NMR spectra of both **2** and **3** exhibit the same splitting pattern with different chemical shifts and support one Et_2O molecule per carboranyl in **2** and two Et_2O molecules per carboranyl in **3**, respectively. In addition, the ^1H NMR spectrum of **2** displays a broad singlet at $\delta = 3.74$ ppm attributable to the cage CH proton, supporting that **2** is a monolithium salt. The ^{13}C NMR data are in line with the results from the corresponding ^1H NMR spectra. The ^{11}B NMR spectra show a 2:3:5 splitting pattern for **2** and a 1:1:1:2:4:1 splitting pattern for **3**, respectively, which are different from those observed in the corresponding ether-functionalized ligands.³

(8) Xie, Z. *Acc. Chem. Res.* **2003**, *36*, 1.

(9) Sheldrick, G. M. *SADABS*: Program for Empirical Absorption Correction of Area Detector Data; University of Göttingen: Germany, 1996.

(10) *SHELXTL V 5.03* Program Package; Siemens Analytical X-ray Instruments, Inc.: Madison, WI, 1995.

Table 1. Crystal Data and Summary of Data Collection and Refinement for 4–8

	4	5·THF	6·toluene	7	8
formula	C ₃₃ H ₆₃ B ₁₀ Cl ₂ LiNO ₄ SiYb	C ₅₄ H ₁₀₂ B ₂₀ Cl ₃ LiN ₂ O ₅ Si ₂ Sm ₂	C ₅₇ H ₁₀₂ B ₂₀ Cl ₃ LiN ₂ O ₄ Si ₂ Yb ₂	C ₃₄ H ₆₂ B ₂₀ Cl ₂ N ₂ Si ₂ Y ₂	C ₃₃ H ₅₇ B ₁₀ ClLiN ₂ OSiSm
cryst size (mm)	0.70 × 0.40 × 0.30	0.50 × 0.50 × 0.08	0.40 × 0.38 × 0.25	0.38 × 0.20 × 0.18	0.30 × 0.21 × 0.11
fw	924.9	1545.8	1611.2	1188.2	826.7
cryst syst	triclinic	monoclinic	monoclinic	triclinic	triclinic
space group	<i>P</i> $\bar{1}$	<i>P</i> 2 ₁ / <i>n</i>	<i>P</i> 2 ₁ / <i>n</i>	<i>P</i> $\bar{1}$	<i>P</i> $\bar{1}$
<i>a</i> , Å	10.482(1)	20.187(1)	20.041(4)	10.201(2)	9.897(3)
<i>b</i> , Å	11.254(1)	17.912(1)	17.837(4)	10.767(2)	11.163(3)
<i>c</i> , Å	21.216(1)	22.299(1)	22.468(5)	12.723(3)	23.517(7)
α , deg	91.24(1)	90	90	82.27(3)	85.20(1)
β , deg	99.03(1)	108.92(1)	109.54(3)	71.48(3)	79.46(1)
γ , deg	92.60(1)	90	90	68.25(3)	68.98(1)
<i>V</i> , Å ³	2468.0(3)	7628.0(5)	7569(3)	1230.5(4)	2384(1)
<i>Z</i>	2	4	4	1	2
<i>D</i> _{calcd} , Mg/m ³	1.245	1.346	1.414	1.603	1.152
radiation (λ), Å	Mo K α (0.71073)	Mo K α (0.71073)	Mo K α (0.71073)	Mo K α (0.71073)	Mo K α (0.71073)
2 θ range, deg	3.6 to 50.0	3.2 to 50.0	3.2 to 50.0	4.0 to 50.0	3.6 to 50.0
μ , mm ⁻¹	2.059	1.703	2.636	3.964	1.338
<i>F</i> (000)	942	3144	1312	582	846
no. of obsd reflns	6365	11942	8011	3494	6113
no. of params refnd	462	785	737	281	443
goodness of fit	1.125	0.986	1.060	1.009	1.065
R1	0.051	0.045	0.101	0.060	0.097
wR2	0.137	0.107	0.244	0.164	0.250

Table 2. Crystal Data and Summary of Data Collection and Refinement for 9–12

	9·0.5(benzene)	10·toluene	11	12
formula	C ₃₂ H ₅₂ B ₁₀ N ₂ SiYb	C ₅₇ H ₁₀₂ B ₂₀ ClLiN ₂ O ₄ Si ₂ Sm ₂	C ₂₁ H ₄₁ B ₁₀ NO ₂ SiYb	C ₅₀ H ₉₄ B ₂₀ Li ₂ N ₂ O ₄ Si ₂ Yb
cryst size (mm)	0.35 × 0.30 × 0.17	0.50 × 0.30 × 0.21	0.35 × 0.15 × 0.08	0.25 × 0.20 × 0.18
fw	774.0	1494.9	648.8	1246.6
cryst syst	monoclinic	triclinic	monoclinic	orthorhombic
space group	<i>P</i> 2 ₁ / <i>n</i>	<i>P</i> $\bar{1}$	<i>P</i> 2 ₁ / <i>n</i>	<i>Pbcn</i>
<i>a</i> , Å	10.726(4)	10.662(2)	12.234(1)	14.893(3)
<i>b</i> , Å	16.012(5)	15.748(3)	15.867(2)	19.577(4)
<i>c</i> , Å	22.289(7)	24.832(5)	15.090(2)	23.115(5)
α , deg	90	104.00(3)	90	90
β , deg	95.86(1)	99.43(3)	90.12(1)	90
γ , deg	90	103.29(3)	90	90
<i>V</i> , Å ³	3808(2)	3829.1(13)	2929.2(5)	6739(2)
<i>Z</i>	4	2	4	4
<i>D</i> _{calcd} , Mg/m ³	1.350	1.297	1.471	1.229
radiation (λ), Å	Mo K α (0.71073)	Mo K α (0.71073)	Mo K α (0.71073)	Mo K α (0.71073)
2 θ range, deg	3.7 to 50.0	3.5 to 50.0	3.7 to 52.0	3.4 to 52.0
μ , mm ⁻¹	2.512	1.625	3.254	1.464
<i>F</i> (000)	1568	1524	1296	2576
no. of obsd reflns	6463	9945	5734	4171
no. of params refnd	416	759	326	364
goodness of fit	0.924	1.051	0.967	1.205
R1	0.061	0.065	0.048	0.068
wR2	0.138	0.179	0.107	0.162

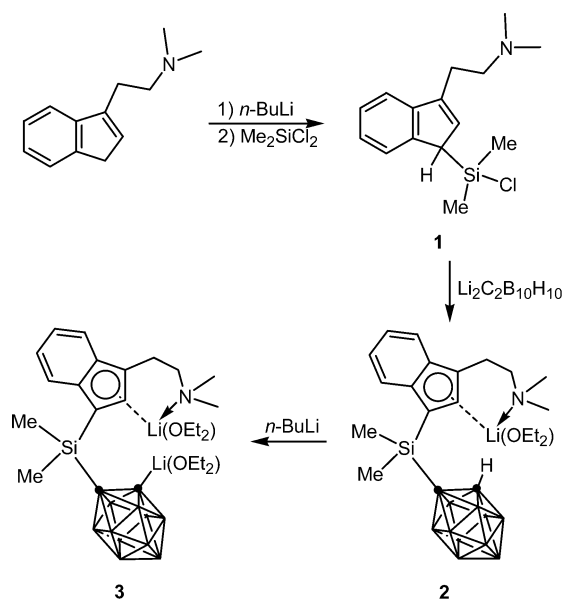
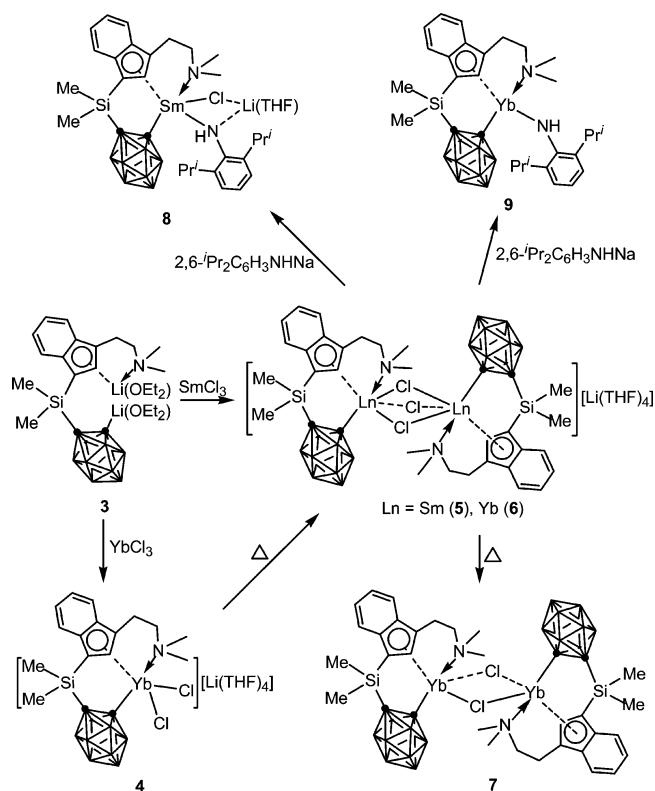
Table 3. Selected Bond Lengths (Å) and Angles (deg)^a

	4	5	6	7	8	9	10	11	12
(Ln)	(Yb)	(Sm)	(Yb)	(Yb)	(Sm)	(Yb)	(Sm)	(Yb)	(Yb)
av Ln–C(ring)	2.668(3)	2.757(3)	2.705(8)	2.617(9)	2.722(14)	2.609(11)	2.732(8)	2.742(8)	2.830(8)
av. Ln–C(cage)	2.520(3)	2.627(3)	2.547(7)	2.438(8)	2.591(14)	2.413(11)		2.510(9)	2.643(9)
av Ln–Cl	2.508(1)	2.793(1)	2.703(1)	2.645(2)	2.752(4)		2.678(3)		
av Ln–N (sidearm)	2.617(3)	2.665(2)	2.619(6)	2.527(7)	2.648(11)	2.457(10)	2.787(8)	2.585(8)	
av C(ring)–Si–C(cage)	107.6(1)	107.0(1)	105.3(3)	104.9(4)	106.8(7)	106.0(5)	102.0(4)	109.3(4)	111.4(4)
av Cent–Ln–C(cage)	105.2	100.2	103.2	104.7	100.3	106.9		103.9	106.4

^a Cent: the centroid of the five-membered ring of the indenyl group.

Reaction with LnCl₃. Treatment of **3** with 1 equiv of YbCl₃ at room temperature gave an ionic complex, [{ η^5 : η^1 : σ -Me₂Si(C₉H₅CH₂CH₂NMe₂)(C₂B₁₀H₁₀)}Yb(μ -Cl)]₂[Li(THF)₄] (**4**), in 78% yield. A THF/toluene solution of **4** was heated at reflux temperature for 2 h to produce, after workup, a complex salt of [{ η^5 : η^1 : σ -Me₂Si(C₉H₅CH₂CH₂NMe₂)(C₂B₁₀H₁₀)}Yb(μ -Cl)]_{1.5}[Li(THF)₄] (**6**) via the elimination of 1 equiv of LiCl. Prolonged heating of a toluene solution of **6** at reflux temperature led to removal of another equivalent of LiCl, generating the

dimeric neutral species [{ η^5 : η^1 : σ -Me₂Si(C₉H₅CH₂CH₂NMe₂)(C₂B₁₀H₁₀)}Yb(μ -Cl)]₂ (**7**) in 58% yield. The samarium analogue of **6**, [{ η^5 : η^1 : σ -Me₂Si(C₉H₅CH₂CH₂NMe₂)(C₂B₁₀H₁₀)}Sm(μ -Cl)]_{1.5}[Li(THF)₄] (**5**), was directly prepared from the reaction of **3** with 1 equiv of SmCl₃ in THF at room temperature. It is noted that no Sm analogue of **4** was isolated even though the reaction conditions and workup procedures were the same, probably owing to steric reasons. These transformations are summarized in Scheme 2.

Scheme 1**Scheme 2**

Complexes 4–7 are paramagnetic species and do not offer much useful NMR information. The ligand-to-solvent ratios were measured by the ¹H NMR spectra of the hydrolysis products of the complexes. Their structures were confirmed by single-crystal X-ray diffraction studies.

The molecular structure of 4 consists of well-separated, alternating layers of the discrete tetrahedral cations [Li(THF)₄]⁺ and anions [$\{\eta^5\text{-}\eta^1\text{-}\sigma\text{-Me}_2\text{Si}(\text{C}_9\text{H}_5\text{CH}_2\text{CH}_2\text{NMe}_2)(\text{C}_2\text{B}_{10}\text{H}_{10})\}\text{YbCl}_2\}$][−]. In the anion, the Yb atom is η^5 -bound to one five-membered ring of the indenyl group and σ -bound to one cage carbon atom, two terminal Cl atoms, and one nitrogen atom from the

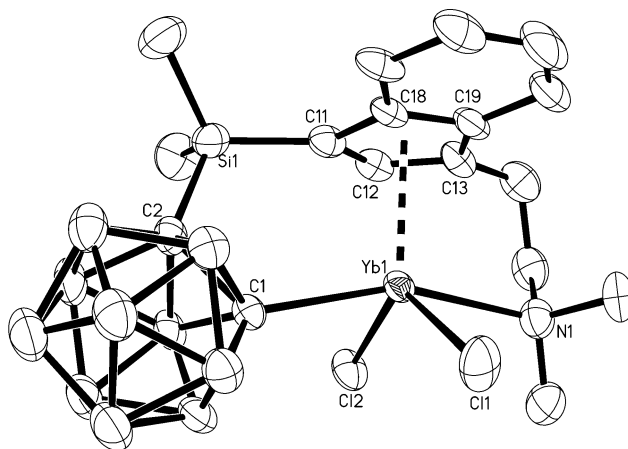


Figure 1. Molecular structure of the anion [$\{\eta^5\text{-}\eta^1\text{-}\sigma\text{-Me}_2\text{Si}(\text{C}_9\text{H}_5\text{CH}_2\text{CH}_2\text{NMe}_2)(\text{C}_2\text{B}_{10}\text{H}_{10})\}\text{YbCl}_2\}$][−] in 4. Selected bond distances (Å) and angles (deg): Yb1–C1 = 2.520(3), Yb1–Cl1 = 2.498(1), Yb1–Cl2 = 2.518(1), Yb1–N1 = 2.617(3), av Yb1–C(ring) = 2.668(3), Cent–Yb1–C1 = 105.2.

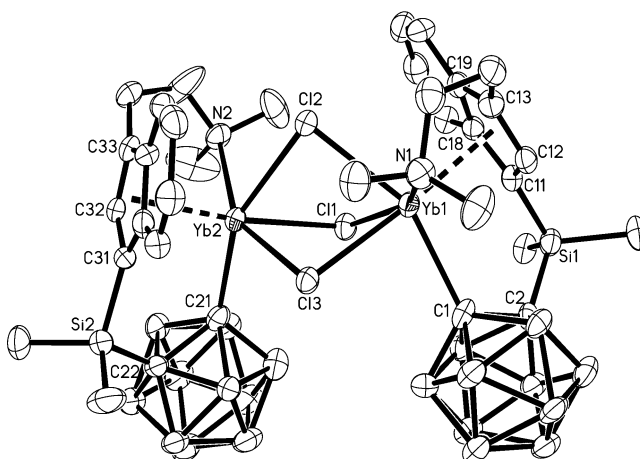


Figure 2. Molecular structure of the anion [$\{\eta^5\text{-}\eta^1\text{-}\sigma\text{-Me}_2\text{Si}(\text{C}_9\text{H}_5\text{CH}_2\text{CH}_2\text{NMe}_2)(\text{C}_2\text{B}_{10}\text{H}_{10})\}\text{Yb}(\mu\text{-Cl})_{1.5}\}$]₂[−] in 6. Selected bond distances (Å) and angles (deg): Yb1–C1 = 2.565(7), Yb2–C21 = 2.529(8), Yb1–Cl1 = 2.678(2), Yb1–Cl2 = 2.726(2), Yb1–Cl3 = 2.718(2), Yb1–N1 = 2.600(6), Yb2–Cl1 = 2.703(2), Yb2–Cl2 = 2.737(2), Yb2–Cl3 = 2.658(2), Yb2–N2 = 2.637(6), av Yb1–C(ring) = 2.704(8), av Yb2–C(ring) = 2.705(8), Cent1–Yb1–C1 = 103.1, Cent2–Yb2–C21 = 103.2.

appended amine group in a four-legged piano stool arrangement (Figure 1). This type of structures is very rare in organolanthanide chemistry, whereas the chlorine-bridged “ate” ones are very common.²

Single-crystal X-ray analyses reveal that 5 and 6 are isostructural and isomorphous, consisting of well-separated, alternating layers of the discrete tetrahedral cations [Li(THF)₄]⁺ and the complex anions [$\{\eta^5\text{-}\eta^1\text{-}\sigma\text{-Me}_2\text{Si}(\text{C}_9\text{H}_5\text{CH}_2\text{CH}_2\text{NMe}_2)(\text{C}_2\text{B}_{10}\text{H}_{10})\}\text{Ln}(\mu\text{-Cl})_{1.5}\}$]₂[−]. The asymmetric unit of 5 contains one THF of solvation, whereas that of 6 shows one toluene of solvation. In the anion, each Ln atom in the dimeric unit is η^5 -bound to one five-membered ring of the indenyl group and σ -bound to one cage carbon atom, three doubly bridging Cl atoms, and one nitrogen atom from the sidearm in a distorted-octahedral coordination environment (Figure 2).

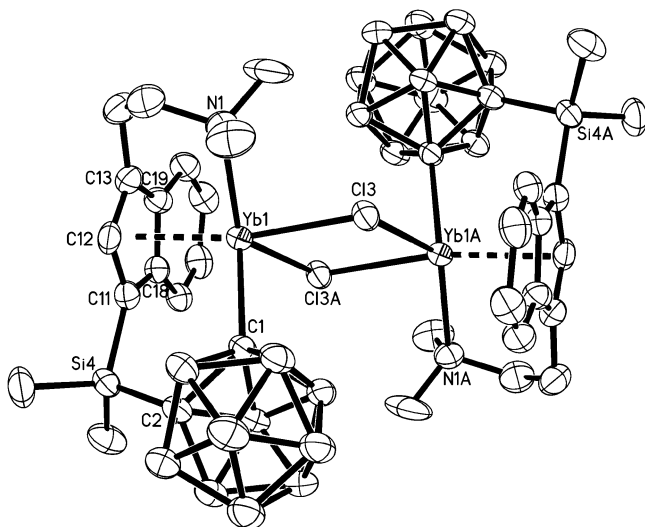


Figure 3. Molecular structure of $[\{\eta^5\text{-}\eta^1\text{-}\sigma\text{-Me}_2\text{Si}(\text{C}_9\text{H}_5\text{CH}_2\text{-CH}_2\text{NMe}_2)(\text{C}_2\text{B}_{10}\text{H}_{10})\}\text{Yb}(\mu\text{-Cl})_2]_2$ (**7**). Selected bond distances (Å) and angles (deg): Yb1–C1 = 2.438(8), Yb1–N1 = 2.527(7), Yb1–Cl3 = 2.675(2), Yb1–Cl3A = 2.614(2), av Yb1–C(ring) = 2.617(9), Cent–Yb1–C1 = 104.7, Yb1–Cl3–Yb1A = 104.54(8).

The solid-state structure of **7** is shown in Figure 3, indicating that it is a centrosymmetric dimer. The coordination environment of each Yb atom is similar to that observed in **4**.

The structural data of **4**, **6**, and **7** (Table 3) show the following trends: (1) for Ln–C(ring, cage) and Ln–N bond distances, **6** > **4** > **7**; and (2) for Ln–Cl distances, **6** > **7** > **4**. These results are understandable since the Yb atom in **6** is eight-coordinate, whereas the seven-coordinate Yb in **4** is bonded to two terminal Cl^- , and the seven-coordinate Yb in **7** is bonded to one bridging Cl^- and one bridging Cl atom, respectively.¹¹ These measured values are close to those found in $[\{\eta^5\text{-}\sigma\text{-Me}_2\text{Si}(\text{C}_9\text{H}_5\text{CH}_2\text{CH}_2\text{OMe})(\text{C}_2\text{B}_{10}\text{H}_{10})\}\text{Ln}(\text{THF})(\mu\text{-Cl})_3\text{Ln}[\eta^5\text{-}\eta^1\text{-}\sigma\text{-Me}_2\text{Si}(\text{C}_9\text{H}_5\text{CH}_2\text{CH}_2\text{OMe})(\text{C}_2\text{B}_{10}\text{H}_{10})]\}_2\{\text{Li}(\text{THF})\}][\text{Li}(\text{THF})_4]$,³ $[\eta^5\text{-}\eta^1\text{-}\sigma\text{-Me}_2\text{Si}(\text{C}_9\text{H}_5\text{CH}_2\text{CH}_2\text{OMe})(\text{C}_2\text{B}_{10}\text{H}_{10})]\}_2\{\text{Li}(\text{THF})\}][\text{Li}(\text{THF})_4]$,³ and $[\eta^5\text{-}\sigma\text{-Me}_2\text{Si}(\text{C}_9\text{H}_6)(\text{C}_2\text{B}_{10}\text{H}_{10})]_2\text{Ln}^-$,⁸ if the differences in Shannon's ionic radii are taken into account.¹¹

The above results show that **4** was converted to **6** and finally to **7** upon heating by eliminating LiCl step by step. Therefore, **4** is suggested to be a kinetic product and **7** is a thermodynamic one. Very low solubility of LiCl in hot toluene provides a driving force for these transformations. Comparing the molecular structure of **7** with that of the ether-functionalized analogue, $[\eta^5\text{-}\eta^1\text{-}\sigma\text{-Me}_2\text{Si}(\text{C}_9\text{H}_5\text{CH}_2\text{CH}_2\text{OMe})(\text{C}_2\text{B}_{10}\text{H}_{10})]\text{Yb}(\text{THF})(\mu\text{-Cl})_2\text{Yb}[\eta^5\text{-}\eta^1\text{-}\sigma\text{-Me}_2\text{Si}(\text{C}_9\text{H}_5\text{CH}_2\text{CH}_2\text{OMe})(\text{C}_2\text{B}_{10}\text{H}_{10})]$,³ steric effects imposed by the coordination of the Me_2N moiety to the Yb atom are very obvious, which reduce the coordination number of the central metal ion by one unit.

Like most lanthanocene chlorides,^{2,3} the chloro groups in the above complexes were able to be replaced by other units via salt metathesis reactions. Treatment of **5** or **6** with 2 equiv of sodium amide gave the "ate" complex $[\eta^5\text{-}\eta^1\text{-}\sigma\text{-Me}_2\text{Si}(\text{C}_9\text{H}_5\text{CH}_2\text{CH}_2\text{NMe}_2)(\text{C}_2\text{B}_{10}\text{H}_{10})]\text{Sm}(\mu\text{-NHC}_6\text{H}_3\text{-2,6-Pr}^i_2)(\mu\text{-Cl})\text{Li}(\text{THF})$ (**8**) or the neutral species $[\eta^5\text{-}$

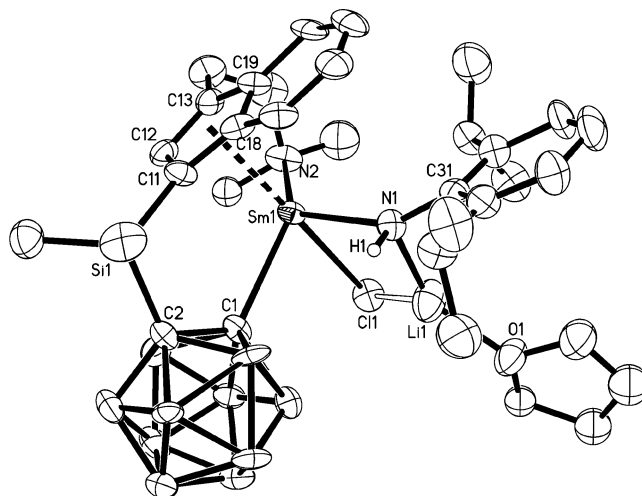


Figure 4. Molecular structure of $[\eta^5\text{-}\eta^1\text{-}\sigma\text{-Me}_2\text{Si}(\text{C}_9\text{H}_5\text{CH}_2\text{-CH}_2\text{NMe}_2)(\text{C}_2\text{B}_{10}\text{H}_{10})]\text{Sm}(\mu\text{-NHC}_6\text{H}_3\text{-2,6-Pr}^i_2)(\mu\text{-Cl})\text{Li}(\text{THF})$ (**8**). Selected bond distances (Å) and angles (deg): Sm1–C1 = 2.591(14), Sm1–N1 = 2.380(12), Sm1–N2 = 2.648(11), Sm1–Cl1 = 2.752(4), Cent–Sm1–C1 = 100.3.

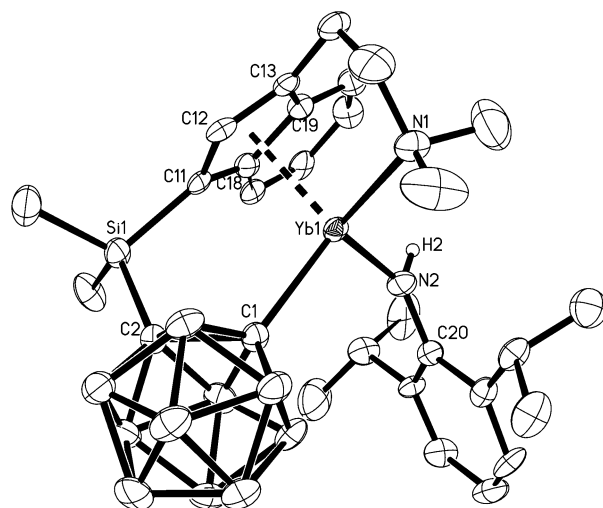


Figure 5. Molecular structure of $[\eta^5\text{-}\eta^1\text{-}\sigma\text{-Me}_2\text{Si}(\text{C}_9\text{H}_5\text{CH}_2\text{-CH}_2\text{NMe}_2)(\text{C}_2\text{B}_{10}\text{H}_{10})]\text{Yb}(\text{NHC}_6\text{H}_3\text{-2,6-Pr}^i_2)$ (**9**). Selected bond distances (Å) and angles (deg): Yb1–C1 = 2.413(11), Yb1–N1 = 2.457(10), Yb1–N2 = 2.140(9), av Yb1–C(ring) = 2.609(11), Cent–Yb1–C1 = 106.9.

$\eta^1\text{-}\sigma\text{-Me}_2\text{Si}(\text{C}_9\text{H}_5\text{CH}_2\text{CH}_2\text{NMe}_2)(\text{C}_2\text{B}_{10}\text{H}_{10})]\text{Yb}(\text{NHC}_6\text{H}_3\text{-2,6-Pr}^i_2)$ (**9**) in good yields, shown in Scheme 2. It is noted that reactions of **6** with alkylating reagents such as CH_3Li , $\text{Me}_3\text{SiCH}_2\text{M}$ ($\text{M} = \text{Li}, \text{K}$), and $\text{Me}_3\text{SiCH}_2\text{MgCl}$ were complicated, and no pure products were isolated. Unlike complex **9**, the coordinated LiCl in **8** cannot be removed by recrystallization from hot toluene, probably because of the larger ionic radius of the Sm^{3+} ion.

Careful examination of the molecular structures of **9** and its ether-functionalized analogue, $[\eta^5\text{-}\eta^1\text{-}\sigma\text{-Me}_2\text{Si}(\text{C}_9\text{H}_5\text{CH}_2\text{CH}_2\text{OMe})(\text{C}_2\text{B}_{10}\text{H}_{10})]\text{Yb}(\text{NHC}_6\text{H}_3\text{-2,6-Pr}^i_2)(\mu\text{-Cl})\text{Li}(\text{THF})_3$,³ may conclude that the coordination of NMe₂ forces the dissociation of LiCl from the central metal ion during recrystallization. Again, steric factors play a role in these transformations.

Single-crystal X-ray analyses confirm the molecular structures of both **8** and **9**, shown in Figures 4 and 5, respectively. **8** exhibits a distorted-trigonal-bipyramidal arrangement of ligands with the Cl atom and the

(11) Shannon, R. D. *Acta Crystallogr.* **1976**, A32, 751.

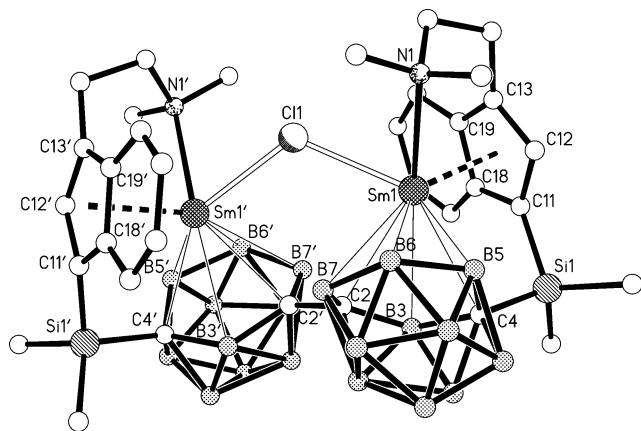
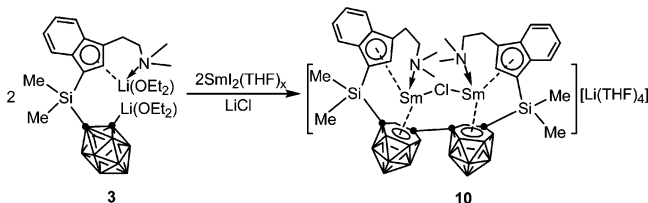


Figure 6. Molecular structure of the anion $[\{\eta^5:\eta^1:\eta^6\text{-Me}_2\text{Si}(\text{C}_9\text{H}_5\text{CH}_2\text{CH}_2\text{NMe}_2)(\text{C}_2\text{B}_{10}\text{H}_{10})\text{Sm}\}_2(\mu\text{-Cl})]^-$ in **10**. Selected bond distances (Å) and angles (deg): C2–C2' = 1.509(10), Sm1–Cl1 = 2.688(3), Sm1'–Cl1 = 2.668(3), Sm1–N1 = 2.709(8), Sm1'–N1' = 2.665(8), av Sm1–C(ring) = 2.731(9), av Sm1–cage atom = 2.815(10), av Sm1'–C(ring) = 2.732(8), av Sm1'–cage atom = 2.804(10), Sm1–Cl1–Sm1' = 120.1(1).

Scheme 3



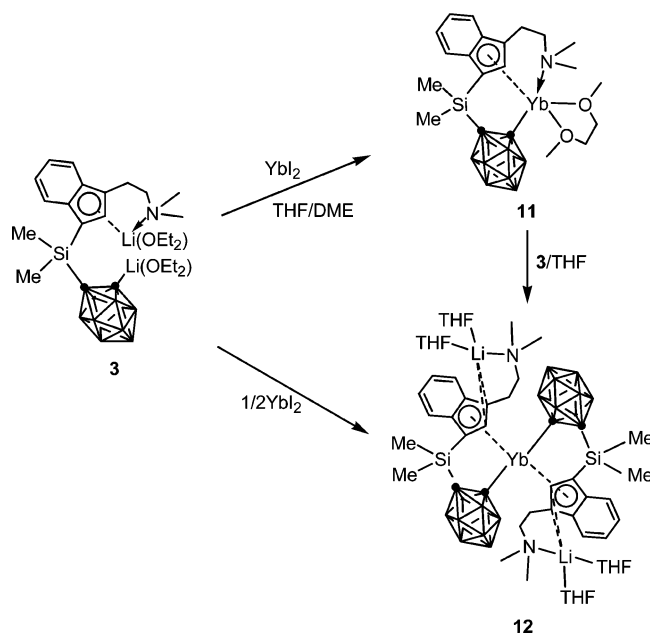
centroid of the five-membered ring occupying the axial positions. On the other hand, **9** shows a distorted-tetrahedral arrangement of ligands. The bond distances observed in **8** and **9** (Table 3) are comparable to the corresponding values found in $[\eta^5:\eta^1:\sigma\text{-Me}_2\text{Si}(\text{C}_9\text{H}_5\text{CH}_2\text{CH}_2\text{OMe})(\text{C}_2\text{B}_{10}\text{H}_{10})]\text{Ln}(\text{NHC}_6\text{H}_3\text{-2,6-Pr}^i_2)(\mu\text{-Cl})\text{Li}(\text{THF})_3$ ³ and other organolanthanide complexes² if the differences in Shannon's ionic radii are taken into account.¹¹

Reaction with LnI₂. Treatment of SmI₂ with 1 equiv of **3** in THF at room temperature gave, after addition of LiCl, the ionic complex $[\{\eta^5:\eta^1:\eta^6\text{-Me}_2\text{Si}(\text{C}_9\text{H}_5\text{CH}_2\text{CH}_2\text{NMe}_2)(\text{C}_2\text{B}_{10}\text{H}_{10})\text{Sm}\}_2(\mu\text{-Cl})][\text{Li}(\text{THF})_4]$ (**10**) as dark red crystals in 43% yield (Scheme 3). This complex was originally isolated from an equimolar reaction of $[\text{Me}_2\text{Si}(\text{C}_9\text{H}_5\text{CH}_2\text{CH}_2\text{NMe}_2)(\text{C}_2\text{B}_{10}\text{H}_{10})]\text{Li}_2(\text{OEt}_2)_2\cdot\text{LiCl}$ with SmI₂ in THF.⁴

A single-crystal X-ray diffraction study confirms that **10** is a trivalent samarium complex, consisting of well-separated, alternating layers of discrete tetrahedral cations $[\text{Li}(\text{THF})_4]^+$ and complex anions $[\{\eta^5:\eta^1:\eta^6\text{-Me}_2\text{Si}(\text{C}_9\text{H}_5\text{CH}_2\text{CH}_2\text{NMe}_2)(\text{C}_2\text{B}_{10}\text{H}_{10})\text{Sm}\}_2(\mu\text{-Cl})]^-$ and shows one toluene of solvation. The coordination geometry of the Sm atoms in **10** is similar to that observed in the ether-functionalized analogue $[\{\eta^5:\eta^1:\eta^6\text{-Me}_2\text{Si}(\text{C}_9\text{H}_5\text{CH}_2\text{CH}_2\text{OMe})(\text{C}_2\text{B}_{10}\text{H}_{10})\text{Sm}\}_2(\mu\text{-Cl})][\text{Li}(\text{THF})_4]$,³ shown in Figure 6. The two *nido*-C₂B₁₀H₁₀ units are connected to each other through a C–C single bond at a distance of 1.509(10) Å, and the dihedral angle between two six-membered C₂B₄ rings is 63.3°.

The average Sm–C(ring) and Sm–cage atom distances of 2.732(8) and 2.809(8) Å in **10** are very

Scheme 4



comparable to the corresponding values observed in $[\{\eta^5:\eta^1:\eta^6\text{-Me}_2\text{Si}(\text{C}_9\text{H}_5\text{CH}_2\text{CH}_2\text{OMe})(\text{C}_2\text{B}_{10}\text{H}_{10})\text{Sm}\}_2(\mu\text{-Cl})][\text{Li}(\text{THF})_4]$ ³ and $[\eta^5:\eta^6\text{-Me}_2\text{Si}(\text{C}_9\text{H}_6)(\text{C}_2\text{B}_{10}\text{H}_{11})]\text{Sm}(\text{THF})_2$.¹² The average Sm–Cl(μ) distance of 2.678(3) Å is slightly longer than the corresponding value of 2.645(4) Å in $[\{\eta^5:\eta^1:\eta^6\text{-Me}_2\text{Si}(\text{C}_9\text{H}_5\text{CH}_2\text{CH}_2\text{OMe})(\text{C}_2\text{B}_{10}\text{H}_{10})\text{Sm}\}_2(\mu\text{-Cl})][\text{Li}(\text{THF})_4]$,³ but is much shorter than the 2.76(1) Å in $[\{\eta^5\text{-C}_5\text{Me}_5\}_2\text{SmCl}_2(\mu\text{-Cl})]^-$ and 2.88(2) Å in $[(\eta^5\text{-C}_5\text{Me}_5)_2\text{Sm}(\mu\text{-Cl})]_3$,¹³ implying that steric repulsion plays an important role.

An equimolar reaction of less reactive YbI₂ with **3** in THF produced, after recrystallization from a toluene/DME solution, the divalent ytterbium complex $[\eta^5:\eta^1:\sigma\text{-Me}_2\text{Si}(\text{C}_9\text{H}_5\text{CH}_2\text{CH}_2\text{NMe}_2)(\text{C}_2\text{B}_{10}\text{H}_{10})]\text{Yb}(\text{DME})$ (**11**) in 66% yield. Treatment of **11** with 1 equiv of **3** gave the ionic complex $[\{(\mu\text{-}\eta^5:\eta^2):\eta^1:\sigma\text{-Me}_2\text{Si}(\text{C}_9\text{H}_5\text{CH}_2\text{CH}_2\text{NMe}_2)(\text{C}_2\text{B}_{10}\text{H}_{10})\}_2\text{Yb}\}\{\text{Li}(\text{THF})_2\}_2]$ (**12**) in 71% yield. Complex **12** was also directly prepared from the reaction of YbI₂ with 2 equiv of **3** in THF. These reactions are summarized in Scheme 4.

The ¹H NMR spectra show the presence of the hybrid ligand and DME in a molar ratio of 1:1 for **11** and support the molar ratio of two THF molecules per hybrid ligand in **12**, respectively. The splitting patterns of the ¹¹B NMR spectra are 2:3 in **11** and 1:2:2 in **12**, respectively. Their solid-state IR spectra display a characteristic B–H absorption of a *closo*-carborane at about 2555 cm^{−1}.

The molecular structure of **11** is shown in Figure 7. The Yb atom is η^5 -bound to the five-membered ring of the indenyl group, σ -bound to the carborane cage carbon atom, and coordinated to one nitrogen atom from the sidearm and two oxygen atoms from one DME molecule in a four-legged piano stool arrangement with a formal coordination number of 7. This is another example showing the differences between $[\text{Me}_2\text{Si}(\text{C}_9\text{H}_5\text{CH}_2\text{CH}_2\text{NMe}_2)(\text{C}_2\text{B}_{10}\text{H}_{10})]\text{Li}_2(\text{OEt}_2)_2\cdot\text{LiCl}$

(12) Xie, Z.; Wang, S.; Yang, Q.; Mak, T. C. W. *Organometallics* **1999**, *18*, 2420.

(13) Evans, W. J.; Drummond, D. K.; Grate, J. W.; Zhang, H.; Atwood, J. L. *J. Am. Chem. Soc.* **1987**, *109*, 3928.

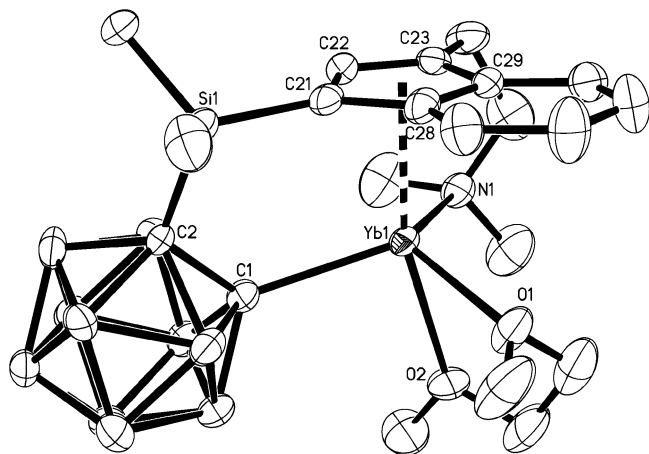


Figure 7. Molecular structure of $[\eta^5:\eta^1:\sigma\text{-Me}_2\text{Si}(\text{C}_9\text{H}_5\text{CH}_2\text{CH}_2\text{NMe}_2)(\text{C}_2\text{B}_{10}\text{H}_{10})]\text{Yb}(\text{DME})$ (**11**). Selected bond distances (Å) and angles (deg): Yb1–C1 = 2.510(9), Yb1–N1 = 2.585(8), Yb1–O1 = 2.388(7), Yb1–O2 = 2.506(6), av Yb1–C(ring) = 2.742(8), Cent–Yb1–C1 = 103.9.

$\text{NMe}_2)(\text{C}_2\text{B}_{10}\text{H}_{10})]^{2-}$ and $[\text{Me}_2\text{Si}(\text{C}_9\text{H}_5\text{CH}_2\text{CH}_2\text{OMe})(\text{C}_2\text{B}_{10}\text{H}_{10})]^{2-}$ in coordination chemistry.

The solid-state structure of **12** was confirmed by single-crystal X-ray analysis, shown in Figure 8. The Yb atom is η^5 -bound to each of two five-membered rings of the indenyl groups and σ -bound to each of two carborane cage carbon atoms in a distorted-tetrahedral geometry, which is very similar to that of $\{[(\mu\text{-}\eta^5:\eta^2):\eta^1:\sigma\text{-Me}_2\text{Si}(\text{C}_9\text{H}_5\text{CH}_2\text{CH}_2\text{OMe})(\text{C}_2\text{B}_{10}\text{H}_{10})]_2\text{Yb}\}\{\text{Li}(\text{THF})_2\}_2$.³

The Yb–C(ring), Yb–C(cage), Yb–N, and Yb–O distances in both **11** and **12** (Table 3) are comparable to the corresponding values observed in $[\eta^5:\eta^1:\sigma\text{-Me}_2\text{Si}(\text{C}_9\text{H}_5\text{CH}_2\text{CH}_2\text{OMe})(\text{C}_2\text{B}_{10}\text{H}_{10})]\text{Yb}(\text{DME})(\text{THF})$,³ $\{[(\mu\text{-}\eta^5:\eta^2):\eta^1:\sigma\text{-Me}_2\text{Si}(\text{C}_9\text{H}_5\text{CH}_2\text{CH}_2\text{OMe})(\text{C}_2\text{B}_{10}\text{H}_{10})]_2\text{Yb}\}\{\text{Li}(\text{THF})_2\}_2$,³ $[\eta^5:\sigma\text{-Pr}^i_2\text{NP}(\text{C}_9\text{H}_6)(\text{C}_2\text{B}_{10}\text{H}_{10})]\text{Yb}(\text{DME})_2$,¹⁴ $[\eta^5:\sigma\text{-Me}_2\text{C}(\text{C}_9\text{H}_6)(\text{C}_2\text{B}_{10}\text{H}_{10})]\text{Yb}(\text{DME})_2$,¹⁵ and other ytterbium(II) complexes¹⁶ if the differences in Shannon's ionic radii are taken into account.¹¹

Conclusion

The amine-functionalized carboranyl-indenyl hybrid ligand shows features similar to the ether-functionalized one. Both of them can prevent lanthanocene chlorides from ligand redistribution reactions via coordinating to the metal ion to meet steric requirements, and offer divalent samarium complexes unusual reactivities, resulting in the formation of unexpected reduction/

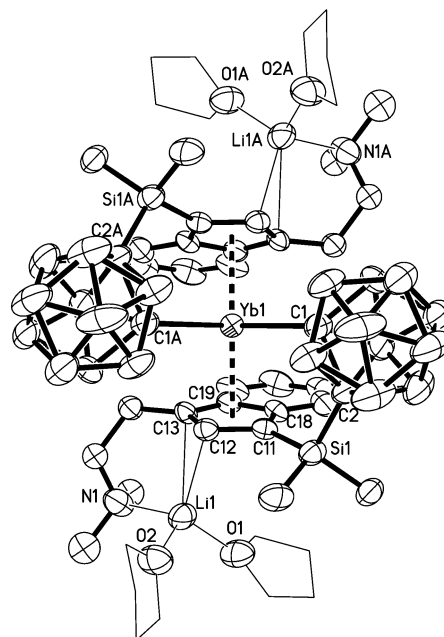


Figure 8. Molecular structure of $\{[(\mu\text{-}\eta^5:\eta^2):\eta^1:\sigma\text{-Me}_2\text{Si}(\text{C}_9\text{H}_5\text{CH}_2\text{CH}_2\text{NMe}_2)(\text{C}_2\text{B}_{10}\text{H}_{10})]_2\text{Yb}\}\{\text{Li}(\text{THF})_2\}_2$ (**12**). Selected bond distances (Å) and angles (deg): Yb1–C1 = 2.643(9), av Yb1–C(ring) = 2.830(8), Li1–C12 = 2.45(2), Li1–C13 = 2.400(9), Cent–Yb1–C1 = 106.4, Cent–Yb1–Cent = 128.5.

coupling products. On the other hand, steric effects imposed by the coordination of NMe_2 to the central metal ion are greater than those resulting from the coordination of OMe , usually leading to the decrease in the coordination number of the central metal ions and the isolation of kinetic products and monomeric neutral species. Such a sidearm effect also results in different structures of early and late lanthanide complexes.

Acknowledgment. The work described in this paper was supported by a grant from the Research Grants Council of the Hong Kong Special Administration Region (Project No. CUHK4026/02P). Z.X. acknowledges the Croucher Foundation for a Senior Research Fellowship Award. S.W. thanks the Excellent Young Scholars Foundation of Anhui Province and the Postdoctoral Fellowship of the Chinese University of Hong Kong.

Supporting Information Available: Crystallographic data and data collection details, atomic coordinates, bond distances and angles, anisotropic thermal parameters, and hydrogen atom coordinates for complexes **4–12** as CIF files. This material is available free of charge via the Internet at <http://pubs.acs.org>.

OM049778+

(14) Wang, H.; Wang, H.; Li, H.-W.; Xie, Z. *Organometallics* **2004**, *23*, 875.

(15) Wang, S.; Yang, Q.; Mak, T. C. W.; Xie, Z. *Organometallics* **2000**, *19*, 334.

(16) Sheng, E.; Wang, S.; Yang, G.; Zhou, S.; Cheng, L.; Zhang, K.; Huang, Z. *Organometallics* **2003**, *22*, 684.